Analysis and power diversity-based cancellation of nonlinear distortions in OFDM systems

Carlos Alexandre Rolim Fernandes, João C.M. Mota, Gérard Favier

Analysis and Power Diversity Based Cancellation of Nonlinear Distortions in OFDM Systems

C. Alexandre R. Fernandes, João C. M. Mota and Gérard Favier

Abstract

One of the main drawbacks of orthogonal frequency division multiplexing (OFDM) systems is the high peak-to-average power ratio (PAPR) of the transmitted signals, which can cause the introduction of inter-carrier interference (ICI) due to the presence of nonlinear power amplifiers (PAs). In this paper, a theoretical analysis of the ICI in nonlinear OFDM systems with polynomial PAs is made. Contrary to other works, this analysis provides an exact description of the nonlinear ICI. Moreover, three receivers for channel estimation and ICI cancellation in OFDM systems with polynomial PAs are proposed, based on the concept of power diversity that consists in re-transmitting the information symbols several times with a different transmission power each time. The transmission powers that minimize the sum of the residual mean square errors (MSEs) provided by the proposed receivers are derived in the case of a third-degree polynomial PA. An important advantage of the proposed receivers is that the optimal transmission powers do not depend on the channel nor the PA coefficients.

Index Terms

OFDM, power amplifier, nonlinear system, channel estimation, inter-carrier interference cancellation.

C. A. R. Fernandes is with the Department of Computer Engineering, Federal University of Ceará, Rua Estanislau Frota s/n, 62010-560, Sobral, Brazil, e-mail: alexandrefernandes@ufc.br. C. A. R. Fernandes is supported by the FUNCAP (Grant No. BP1-0031-00106.01.00/10).

J. C. M. Mota is with the Department of Teleinformatics Engineering, Federal University of Ceará, Campus do Pici, 60.755-640, 6007 Fortaleza, Brazil, e-mail: mota@gtel.ufc.br

G. Favier is with the I3S Laboratory, University of Nice-Sophia Antipolis and CNRS, 2000 route des Lucioles, BP 121, 06903, Sophia-Antipolis Cedex, France, e-mail: favier@i3s.unice.fr

I. INTRODUCTION

Orthogonal frequency division multiplexing (OFDM) has many applications in the area of wireless communications [1]–[4]. One of the main drawbacks of OFDM is that the transmitted signals are characterized by a high peak-to-average power ratio (PAPR) [1], [2]. Due to the presence of nonlinear devices such as power amplifiers (PAs), a high PAPR causes the introduction of nonlinear inter-carrier interference (ICI) in the received signals if a high input back-off (IBO) is not used, which can significantly deteriorate the recovery of the information symbols. The IBO is defined as the ratio between the PA saturation power, i.e. the input power corresponding to the maximum output power, and the average PA input power. A high IBO results in a low-power efficiency of the PA and a low signal to noise ratio (SNR) at the receiver.

In this paper, the PA is modeled as a polynomial with complex-valued frequency-independent coefficients. This model, also called a quasi-memoryless polynomial model, is widely used in the literature to characterize PA amplitude and phase distortions (AM/AM and AM/PM conversions) when the PA memory is short compared to the time variations of the input signal envelope [5]–[12]. In fact, the present work can be extended to the case where the PA is modeled as a Hammerstein system [8], as long as the cyclic prefix has an appropriate length. That is due to the fact that the linear filter of the PA can be combined with the impulse response of the wireless channel. Moreover, the receivers proposed in this work can be extended to the case of PAs with frequency-dependent coefficients. However, due to simplicity reasons, we will assume that the PA coefficients are frequency-independent.

The first contribution of this paper consists in an exact characterization of the ICI in an OFDM system with a polynomial PA. Theoretical analysis of OFDM systems with nonlinear memoryless PAs has been the subject of several studies in the literature [3], [4], [7], [11]–[14]. However, most of these works approximate the probability density function of the transmitted signal by a complex Gaussian function. This approximation holds when the number of sub-carriers is large. Contrary to previous works, our analysis gives an exact characterization of nonlinear ICI. The original contributions of this analysis are the following. We first derive a new exact closed-form expression for the nonlinear ICI in terms of the frequency-domain data symbols. Then, we obtain new expressions for the variance of the third-order ICI and for the cross-correlation between one data symbol and the third-order ICI corresponding to the same subcarrier. The main motivation for deriving these second-order statistics of the nonlinear ICI is that they are used by the receivers proposed in this paper. Moreover, these statistics provide important information about the statistical behavior of the nonlinear OFDM system. It should be highlighted that third-degree

polynomials have been widely used to model nonlinear PAs [8], [15]–[17]. The ICIs considered in [3], [4], [7], [11]–[14] are not the same as in our manuscript and, as a consequence, the ICI variances and the cross-correlations between data symbols and ICIs are different as well.

The second contribution of the paper is the proposition of one receiver for ICI cancellation and two receivers for joint ICI cancellation and wireless channel frequency response (CFR) estimation in OFDM systems with polynomial PAs. These receivers are based on three different scenarios regarding the availability of channel state information (CSI) at the receiver. In the first scenario, it is assumed that CSI is available at the receiver, that is, the receiver a priori knows the wireless CFR and the PA coefficients. In the second scenario, it is assumed that the receiver does not have CSI, while in a third scenario, it is assumed that the receiver has a partial CSI, that is, the receiver a priori knows the PA coefficients, but not the CFR. This last case is justified by the fact that the PA coefficients can be estimated by the transmitter and this information can be sent to the receiver through a control channel during the system initialization [18]. In these three scenarios, it is assumed that the transmitter does not know the wireless CFR.

The proposed receivers are based on the concept of power diversity, which consists in re-transmitting the information symbols several times with a different transmission power each time. The power diversity induces a multi-channel representation, allowing a perfect recovery of the information symbols in the noiseless case. The main drawback of this approach is that the transmission rate is divided by the repetition factor, i.e. the number of times that every symbol is transmitted. However, in the case of a third-order PA, which is the case of main interest, we can use a repetition factor equal to 2.

Signal pre-distortion [8], [15], [16], [19], [20] and PAPR reduction [21], [22] are other popular methods used to reduce the effects of PA nonlinearities in communication systems. Compared with these methods, our approach of compensating the nonlinear distortions at the receiver has the advantage of taking other channel nonlinearities into account, contrary to pre-distortion and PAPR reduction schemes that generally compensate the nonlinear distortions of a single nonlinear block. Moreover, some authors have found that better ICI mitigation results are attained when we focus our efforts on the reception [23]. It should be highlighted that ICI cancellation techniques at the receiver can be used concurrently with pre-distortion and PAPR reduction methods.

Techniques for nonlinear ICI rejection at the receiver based on iterative methods [24]–[27], statistical approaches [28], [29] and nonlinear adaptive filtering [30] have been proposed. An iterative receiver for nonlinear space-division multiple access (SDMA) OFDM systems consisting in the estimation and cancellation of nonlinear distortions at the receiver was proposed in [18], [31], based on an iterative

technique for maximum likelihood detection of nonlinearly distorted symbols [32].

Another contribution of the present paper is the determination of optimal transmission powers that minimize the residual mean square error (MSE) provided by the proposed receivers, in the case of a third-degree polynomial PA and a repetition factor equal to 2. An important property of the proposed receivers is that the optimal transmission powers are constant, that is, they do not depend on channel and noise conditions, which is not the case when no ICI cancellation is made at the receiver [33], [34].

The rest of the paper is organized as follows. Section II describes the system model considered in this work. In Section III, the nonlinear ICI analysis is made. Section IV presents the power diversity based transmission scheme and three receivers are derived. In Section V, optimal transmission powers are established. Section VI evaluates the performance of the proposed receivers by means of computer simulations and some conclusions and perspectives are drawn in Section VII.

Notation: lower-case letters (x) denote scalar variables, bold lower-case letters ($\mathbf{x}$) denote column vectors and bold upper-case letters ($\mathbf{X}$) denote matrices. Overlined variables correspond to frequency-domain variables. $[\mathbf{x}]_i$ represents the i^{th} element of $\mathbf{x}$, $[\mathbf{X}]_{i,j}$ is the $(i,j)^{th}$ element of $\mathbf{X}$, diag $[\mathbf{x}]$ denotes the diagonal matrix built from the vector $\mathbf{x}$ and $[\mathbf{X}]_{i,\cdot}$ represents the i^{th} row of $\mathbf{X}$. Moreover, $\mathbf{X}^{\dagger}$ and $\mathbf{X}^{*}$ denote the Moore-Penrose pseudo-inverse and the complex conjugate of $\mathbf{X}$, respectively. The function cir(x,N), for $-N+1 \leq x \leq N$ is defined as follows: cir$(x,N) = x$ if $1 \leq x \leq N$ and cir$(x,N) = x+N$ if $-N+1 \leq x \leq 0$.

II. System Model

A simplified scheme of the discrete-time equivalent baseband OFDM system used in this work is shown in Fig. 1. Let us denote by N the number of subcarriers, $\bar{s}_{i,n}$ the frequency-domain data symbol at the n^{th} subcarrier and i^{th} symbol period, for $1 \leq n \leq N$ and $1 \leq i \leq I$, I being the number of symbol periods, and $\bar{\mathbf{s}}(i) = [\bar{s}_{i,1} \cdots \bar{s}_{i,N}]^T \in \mathbb{C}^{N \times 1}$ the vector containing the N data symbols of the i^{th} symbol period. The frequency-domain data symbols $\bar{s}_{i,n}$ are assumed to be independent and identically distributed (i.i.d.), with a uniform distribution over a quadrature amplitude modulation (QAM) or a phase-shift keying (PSK) alphabet. Moreover, it is assumed that the transmitter does not have CSI. Thus, we consider that all the subcarriers have the same transmission power.

The i^{th} time-domain OFDM symbol is obtained by taking the Inverse Discrete Fourier Transform (IDFT) of frequency-domain data symbols, that is:

$$s_{i,n'} = \frac{1}{\sqrt{N}} \sum_{n=1}^{N} e^{\jmath 2\pi (n-1)(n'-1)/N} \bar{s}_{i,n}, \tag{1}$$

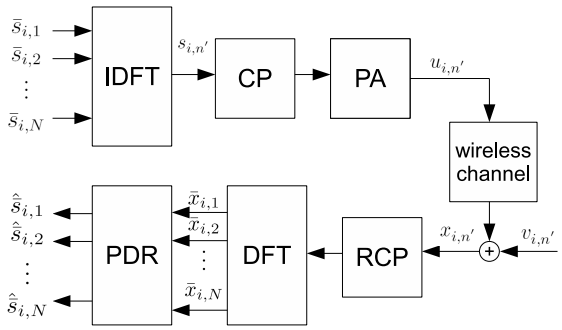

Fig. 1. Discrete-time equivalent baseband OFDM system.

for $1 \leq n^{'} \leq N$, which can be written in matrix form as: $\mathbf{s}(i) = \mathbf{F}\ \bar{\mathbf{s}}(i)$, where $\mathbf{s}(i) = [s_{i,1} \cdots s_{i,N}]^T \in \mathbb{C}^{N\times 1}$ is the i^{th} time-domain symbol vector and $\mathbf{F} \in \mathbb{C}^{N\times N}$ is the IDFT matrix of order N, with $[\mathbf{F}]_{p,q} = \frac{1}{\sqrt{N}} e^{\jmath 2\pi (p-1)(q-1)/N}$, for $1 \leq p, q \leq N$. After the IDFT block, a cyclic prefix (CP) of length M_{cp} is inserted in order to avoid intersymbol interference (ISI). The time-domain symbol vector with the cyclic prefix is given by $\mathbf{s}^{(cp)}(i) = [s_{i,(N-M_{cp}+1)} \cdots s_{i,N}\ \ \mathbf{s}(i)^T]^T \in \mathbb{C}^{(N+M_{cp})\times 1}$. When the PA is linear, the cyclic prefix can avoid ISI and ICI, ensuring the orthogonality between the subcarriers. However, as shown in the sequel, for a nonlinear PA, some ICI is introduced in the received signals, even when a cyclic prefix is used.

The time-domain symbols with the CP are then amplified by a PA that is modeled as a polynomial of degree $2K+1$ [5], [8], [9], $K+1$ being the number of polynomial coefficients. Denoting by $u_{i,n'}$ $(1 \leq n^{'} \leq N)$ the output of the PA, we have:

$$\begin{aligned} u_{i,n'} &= \sum_{k=0}^{K} c_{2k+1} |s_{i,n'}|^{2k} s_{i,n'} \\ &= \sum_{k=0}^{K} c_{2k+1} \psi_{2k+1}(s_{i,n'}), \end{aligned} \tag{2}$$

where c_{2k+1}, for $0 \leq k \leq K$, are the equivalent baseband polynomial coefficients and the operator $\psi_{2k+1}(\cdot)$ is defined as $\psi_{2k+1}(a) = |a|^{2k} a$. Note that, as the PA model is memoryless, the PA output also has a cyclic prefix. The equivalent baseband polynomial model (2) includes only odd-order power terms with one more non-conjugated term than conjugated terms because the other products of input signals correspond to spectral components lying outside the channel bandwidth, and can therefore be eliminated by passband filtering [35]. Besides, as earlier mentioned, the receivers proposed in this work can be extended to the case of PAs with frequency-dependent coefficients. However, we will use the model (2)

through this work for simplicity reasons.

The PA output is transmitted through a frequency-selective fading wireless channel with impulse response denoted by h_m, for $m = 0, 1, ..., M$, where M is the wireless channel delay spread, and an additive white Gaussian noise (AWGN) of variance σ^2 is assumed at the channel output. At the receiver, the CP is removed from the time-domain received signal $x_{i,n'}$ ($1 \leq n' \leq N + M_{cp}$). Thus, assuming that the length of the cyclic prefix is greater than or equal to the channel delay spread ($M_{cp} \geq M$), the wireless channel can be represented by a circular convolution:

$$x_{i,(n'+M_{cp})} = \sum_{m=0}^{M} h_m u_{i,\text{cir}(n'-m,N)} + v_{i,(n'+M_{cp})}, \tag{3}$$

for $1 \leq n' \leq N$, where $v_{i,(n'+M_{cp})}$ is the AWGN component. Equation (3) can also be expressed in matrix form as:

$$\mathbf{x}(i) = \mathbf{H}\mathbf{u}(i) + \mathbf{v}(i), \tag{4}$$

where $\mathbf{x}(i) = [x_{i,(M_{cp}+1)} \cdots x_{i,(M_{cp}+N)}]^T \in \mathbb{C}^{N\times 1}$, $\mathbf{u}(i) = [u_{i,1} \cdots u_{i,N}]^T \in \mathbb{C}^{N\times 1}$, $\mathbf{v}(i) = [v_{i,(M_{cp}+1)} \cdots v_{i,(N+M_{cp})}]^T \in \mathbb{C}^{N\times 1}$ and $\mathbf{H} \in \mathbb{C}^{N\times N}$ is the circulant matrix constructed from the channel impulse response h_m ($0 \leq m \leq M$), with $[\mathbf{H}]_{i,j} = h_{i-j}$ if $0 \leq i - j \leq M$, $[\mathbf{H}]_{i,j} = h_{i-j+N}$ if $i - j \leq M - N$ and $[\mathbf{H}]_{i,j} = 0$ otherwise, for $1 \leq i, j \leq N$.

The DFT of the received signals is then calculated as:

$$\bar{\mathbf{x}}(i) = \mathbf{F}^*\mathbf{x}(i) = \mathbf{F}^*\mathbf{H}\mathbf{F}\bar{\mathbf{u}}(i) + \bar{\mathbf{v}}(i). \tag{5}$$

where $\bar{\mathbf{x}}(i) \in \mathbb{C}^{N\times 1}$ is the vector of frequency-domain received signals at the i^{th} symbol period, $\bar{\mathbf{u}}(i) = \mathbf{F}^*\mathbf{u}(i)$ is the frequency-domain version of $\mathbf{u}(i)$ and $\bar{\mathbf{v}}(i) = \mathbf{F}^*\mathbf{v}(i) \in \mathbb{C}^{N\times 1}$ is the frequency-domain noise vector, which is also white and Gaussian with the same covariance $\sigma^2\mathbf{I}_N$ as $\mathbf{v}(i)$, $\mathbf{I}_N$ being the identity matrix of order N.

It is well known that a circulant matrix is diagonalized by a IDFT matrix. Thus, we can write: $\mathbf{\Lambda} = \mathbf{F}^*\mathbf{H}\mathbf{F}$, where $\mathbf{\Lambda} \in \mathbb{C}^{N\times N}$ is a diagonal matrix containing the eigenvalues of $\mathbf{H}$ [36] and the n^{th} eigenvalue of $\mathbf{H}$, denoted by $\lambda_n = [\mathbf{\Lambda}]_{n,n}$, represents the CFR at the n^{th} subcarrier. By defining: $\boldsymbol{\psi}_{2k+1}(\mathbf{a}) = [\psi_{2k+1}(a_1) \cdots \psi_{2k+1}(a_N)]^T \in \mathbb{C}^{N\times 1}$, for $\mathbf{a} = [a_1 \cdots a_N]^T \in \mathbb{C}^{N\times 1}$, and using (2), we can rewrite (5) as:

$$\bar{\mathbf{x}}(i) = \mathbf{\Lambda} \sum_{k=0}^{K} c_{2k+1}\mathbf{F}^*\boldsymbol{\psi}_{2k+1}(\mathbf{s}(i)) + \bar{\mathbf{v}}(i). \tag{6}$$

Defining $\bar{\boldsymbol{\psi}}_{2k+1}(\mathbf{s}(i)) = \mathbf{F}^{*}\boldsymbol{\psi}_{2k+1}(\mathbf{s}(i)) \in \mathbb{C}^{N\times 1}$ as the frequency-domain version of $\boldsymbol{\psi}_{2k+1}(\mathbf{s}(i))$, $\bar{\xi}_{2k+1}(i,n) = [\bar{\boldsymbol{\psi}}_{2k+1}(\mathbf{s}(i))]_n$ and $\bar{\boldsymbol{\phi}}_{i,n} = [\bar{s}_{i,n} \quad \bar{\xi}_3(i,n)\cdots\bar{\xi}_{2K+1}(i,n)]^T \in \mathbb{C}^{(K+1)\times 1}$, the frequency-domain received signal $\bar{x}_{i,n} = [\bar{\mathbf{x}}(i)]_n$ can be expressed as:

$$\bar{x}_{i,n} = \lambda_n \mathbf{c}^T \bar{\boldsymbol{\phi}}_{i,n} + \bar{v}_{i,n}, \tag{7}$$

where $\mathbf{c} = [c_1 \quad c_3 \cdots c_{2K+1}]^T \in \mathbb{C}^{(K+1)\times 1}$ and $\bar{v}_{i,n}$ is the corresponding noise component in the frequency domain.

Equation (7) shows that the frequency-domain received signal $\bar{x}_{i,n}$ equals a scaled version of the frequency-domain data symbol $\lambda_n c_1 \bar{s}_{i,n}$ plus weighted nonlinear ICI terms $\sum_{k=1}^{K} \lambda_n c_{2k+1}\bar{\xi}_{2k+1}(i,n)$, plus a noise term, with $\bar{\xi}_{2k+1}(i,n)$ representing the $(2k+1)$th-order ICI at the n^{th} subcarrier and i^{th} symbol period. Moreover, we can note that $\bar{x}_{i,n}$ is not corrupted by interferences from other symbol periods. In the sequel, we develop a closed-form expression and a statistical characterization of the nonlinear ICI $\bar{\xi}_{2k+1}(i,n)$ and, then, several techniques for eliminating the nonlinear ICI and removing the scalar factor $\lambda_n c_1$ are presented. The proposed receivers, called power diversity receivers (PDRs), are carried out after the DFT operation.

Moreover, without loss of generality, we can assume that $c_1 = 1$, as the linear PA coefficient c_1 can be absorbed by the CFR λ_n and the other PA coefficients $c_3, \ldots, c_{2K+1}$ can be normalized by c_1 without changing the value of $\bar{x}_{i,n}$ in (7).

III. Nonlinear ICI Analysis

In this section, an analytical expression of the nonlinear ICI in an OFDM system with a polynomial PA is developed. This expression, contrary to the ones presented in previous works [3], [4], [11], [13], [14], corresponds to an exact description of the nonlinear ICI. After deriving a closed-form expression for the nonlinear ICI in terms of the frequency-domain data symbols, we obtain new expressions for the variance of the third-order ICI and for the correlation between one data symbol and the third-order ICI corresponding to the same subcarrier. These second-order statistics of the nonlinear ICI provide important information about the statistical behavior of the nonlinear OFDM system and are used by some of the ICI cancellation techniques proposed in Section IV.

A. Closed-Form Expression for the Nonlinear ICI

From (1), we may write:

$$\psi_{2k+1}(s_{i,n'}) = |s_{i,n'}|^{2k} s_{i,n'} = \frac{1}{N^{\frac{2k+1}{2}}} \sum_{n_1=1}^{N} \sum_{n_2=1}^{N} \cdots \sum_{n_{2k+1}=1}^{N} e^{\jmath 2\pi \left(-\sum_{j=1}^{k} n_j + \sum_{j=k+1}^{2k+1} n_j - 1\right)(n'-1)/N} \prod_{j=1}^{k} \bar{s}^{*}_{i,n_j} \prod_{j=k+1}^{2k+1} \bar{s}_{i,n_j}. \quad (8)$$

The $(2k+1)^{th}$ order ICI $\bar{\xi}_{2k+1}(i,n)$ is calculated by taking the DFT of (8) in the following way:

$$\bar{\xi}_{2k+1}(i,n) = \frac{1}{N^{k+1}} \sum_{n'=1}^{N} \sum_{n_1=1}^{N} \cdots \sum_{n_{2k+1}=1}^{N} e^{-\jmath 2\pi (n'-1)(n-1)/N} e^{\jmath 2\pi \left(-\sum_{j=1}^{k} n_j + \sum_{j=k+1}^{2k+1} n_j - 1\right)(n'-1)/N} \prod_{j=1}^{k} \bar{s}^{*}_{i,n_j} \prod_{j=k+1}^{2k+1} \bar{s}_{i,n_j}, \quad (9)$$

which leads to:

$$\bar{\xi}_{2k+1}(i,n) = \frac{1}{N^{k+1}} \sum_{n_1=1}^{N} \cdots \sum_{n_{2k+1}=1}^{N} \left(\sum_{n'=1}^{N} e^{\jmath 2\pi (n'-1)(-\sum_{j=1}^{k} n_j + \sum_{j=k+1}^{2k+1} n_j - n)/N} \right) \prod_{j=1}^{k} \bar{s}^{*}_{i,n_j} \prod_{j=k+1}^{2k+1} \bar{s}_{i,n_j}. \quad (10)$$

Using the following result:

$$\sum_{n'=1}^{N} e^{\jmath 2\pi (n'-1)(-\sum_{j=1}^{k} n_j + \sum_{j=k+1}^{2k+1} n_j - n)/N} = \begin{cases} 0, & \text{if} \quad -\sum_{j=1}^{k} n_j + \sum_{j=k+1}^{2k+1} n_j - n \neq Np, \\ N, & \text{if} \quad -\sum_{j=1}^{k} n_j + \sum_{j=k+1}^{2k+1} n_j - n = Np, \end{cases} \quad (11)$$

for $p \in \mathbb{Z}$, we can reexpress the $(2k+1)$th order ICI on the nth subcarrier as:

$$\bar{\xi}_{2k+1}(i,n) = \frac{1}{N^{k}} \sum_{n_1=1}^{N} \cdots \sum_{n_{2k}=1}^{N} \left(\prod_{j=1}^{k} \bar{s}^{*}_{i,n_j} \right) \left(\prod_{j=k+1}^{2k} \bar{s}_{i,n_j} \right) \bar{s}_{i,\mathrm{cir}(n+\Sigma_{j=1}^{k} n_j - \Sigma_{j=k+1}^{2k} n_j, N)}. \quad (12)$$

In particular, the third-order ICI is given by:

$$\bar{\xi}_{3}(i,n) = \frac{1}{N} \sum_{n_1=1}^{N} \sum_{n_2=1}^{N} \bar{s}^{*}_{i,n_1} \bar{s}_{i,n_2} \bar{s}_{i,\mathrm{cir}(n+n_1-n_2,N)}. \quad (13)$$

Eqs. (12) and (13) are exact closed-form expressions for the nonlinear ICI that only depend on the number of subcarriers and the data symbols. Besides, it should be remarked that the nonlinear ICI of the n^{th} subcarrier depends on the information symbols of all the other subcarriers, which means that each subcarrier interferes on all the other subcarriers. This phenomenon can be viewed as a consequence of the spectral broadening caused by the nonlinearity. Note also that, eq. (12) reduces to $\bar{\xi}_{1}(i,n) = \bar{s}_{i,n}$ for $k = 0$.

B. Second-Order Statistics of the Nonlinear ICI

In this subsection, we develop expressions for second-order statistics of the nonlinear ICI based on the relationships established in Subsection III-A. These statistics provide us important information about the nonlinear ICI and are used by some of the techniques proposed in Section IV. However, due to the high complexity of these expressions and to the fact that we are mainly interested in third-order modeling of the PA, as currently considered in the literature [8], [15]–[17], the expressions developed in the sequel concern only third-order ICI. Specifically, we derive the expressions for the variance of the third-order ICI and the cross-correlation between one data symbol and the third-order ICI corresponding to the same subcarrier.

Let us denote the correlation between two nonlinear ICIs associated with the n^{th} subcarrier as: $r_n(k_1,k_2)=\mathbb{E}[\bar{\xi}_{2k_1+1}(i,n)\bar{\xi}^*_{2k_2+1}(i,n)]$, for $0\leq k_1,k_2\leq K$. By defining $\mu_j=\mathbb{E}\left[|\bar{s}_{i,n}|^j\right]$, $\varrho_j=\mathbb{E}\left[\bar{s}^j_{i,n}\right]$ and $\varrho_{l,j}=\mathbb{E}\left[\bar{s}^l_{i,n}[\bar{s}^*_{i,n}]^j\right]$, we have $\varrho_1=0$, $\varrho_3=0$ and $\varrho_{2,1}=0$ for uniform i.i.d. Q-QAM and Q-PSK inputs, and $r_n(0,0)=\mathbb{E}[|\bar{s}_{i,n}|^2]=\mu_2$. Using (13) gives:

$$\begin{aligned} r_n(1,0) &= \mathbb{E}\left[\bar{\xi}_3(i,n)\bar{s}^*_{i,n}\right] \\ &= \frac{1}{N}\sum_{n_1=1}^{N}\sum_{n_2=1}^{N}\mathbb{E}\left[\bar{s}^*_{i,n_1}\bar{s}_{i,n_2}\bar{s}_{i,\text{cir}(n-n_2+n_1,N)}\bar{s}^*_{i,n}\right]. \end{aligned} \tag{14}$$

where

$$\mathbb{E}\left[\bar{s}^*_{i,n_1}\bar{s}_{i,n_2}\bar{s}_{i,\text{cir}(n-n_2+n_1,N)}\bar{s}^*_{i,n}\right]=\begin{cases}\mu_4, & \text{if} \quad n_1=n_2=n,\\ \mu_2^2, & \text{if} \quad n_1=n_2\neq n \quad \text{or} \quad n_2=n\neq n_1,\\ \varrho_2^2, & \text{if} \quad n_1=n \quad \text{and} \quad n_2=\text{cir}(n+N/2,N),\\ 0, & \text{otherwise.}\end{cases} \tag{15}$$

This allows us to rewrite (14) as:

$$r_n(1,0)=\frac{1}{N}\left[\mu_4+2(N-1)\mu_2^2+\varrho_2^2\right]=r_n(0,1). \tag{16}$$

It can then be concluded that the third-order ICI is correlated with the data-symbol associated with the same subcarrier.

Assuming that N is even, the variance of $\bar{\xi}_3(i,n)$, defined as:

$$\begin{aligned} r_n(1,1) &= \mathbb{E}\left[\bar{\xi}_3(i,n)\bar{\xi}^*_3(i,n)\right] \\ &= \frac{1}{N^2}\sum_{n_1=1}^{N}\sum_{n_2=1}^{N}\sum_{n_3=1}^{N}\sum_{n_4=1}^{N}\mathbb{E}\left[\bar{s}^*_{i,n_1}\bar{s}_{i,n_2}\bar{s}_{i,\text{cir}(n-n_2+n_1,N)}\bar{s}_{i,n_3}\bar{s}^*_{i,n_4}\bar{s}^*_{i,\text{cir}(n-n_4+n_3,N)}\right], \end{aligned} \tag{17}$$

is given by:

$$r_n(1,1) = \frac{1}{N^2}\left[\mu_6 + 9(N-1)\mu_2^2\mu_4 + 6(N-1)(N-2)\mu_2^3 + 9(N-2)\varrho_2^2\mu_2 + 6\varrho_2\varrho_{31}\right]. \quad (18)$$

The derivation of (18) is omitted due to a lack of space. Note that $r_n(0,0)$, $r_n(1,0)$ and $r_n(1,1)$ are independent of the subcarrier number, which allows us to omit the index n in these correlations.

When N is large, eqs. (16) and (18) can be approximated respectively by:

$$r(1,0) \cong 2\mu_2^2 \quad \text{and} \quad r(1,1) \cong 6\mu_2^3. \quad (19)$$

That corresponds to the values of $r(1,0)$ and $r(1,1)$ when the time-domain signals $s_{i,n}$ are circular symmetric complex Gaussian variables. The expressions (19) can then be viewed as a particular case of (16) and (18) that holds only when the number of subcarriers is high.

We claim that (16) and (18) can be used to derive theoretical symbol error probability expressions for OFDM systems with third-degree polynomial PAs, when N is not large. This issue will be considered in a future work.

In [3], [4], [7], [11]–[14], the ICI expressions are not the same as those obtained in the present work, which explains why the ICI variances and the cross-correlation between one data symbol and the ICI are also different from the ones above presented.

IV. Power Diversity-based Receivers (PDRs)

In subsection IV-A, we first introduce the concept of power diversity by presenting a transmission scheme that consists in re-transmitting the information symbols several times with different transmission powers. Then, three receivers based on the proposed power diversity transmission scheme are presented considering three different scenarios. In Subsection IV-B, it is assumed that the CSI is available at the receiver, that is, the wireless CFR and PA coefficients are known at the receiver. In Subsection IV-C, the receiver does not have CSI, that is, the wireless CFR and the PA coefficients are unknown at the receiver, and in Subsection IV-D, it is assumed that partial CSI (PCSI) is available at the receiver, that is, the PA coefficients are known at the receiver, but the wireless CFR is unknown.

A. Transmission Scheme

The i^{th} frequency-domain information symbol $\bar{s}_{i,n}$ at the n^{th} subcarrier ($1 \leq n \leq N$, $1 \leq i \leq I$) is transmitted L times with transmission power factors $P_1, ..., P_L$, as follows:

$$\bar{s}^{(pd)}_{((i-1)L+l),n} = \sqrt{P_l}\,\bar{s}_{i,n}, \quad \text{for} \quad 1 \leq l \leq L, \quad (20)$$

where $\bar{s}^{(pd)}_{((i-1)L+l),n}$ is the transmitted frequency-domain symbol associated with the n^{th} subcarrier and $((i-1)L+l)^{th}$ symbol period. Note that the transmission power factors $P_1, ..., P_L$ are the same for all the subcarriers.

For each subcarrier, one frequency-domain information symbol $\bar{s}_{i,n}$ generates a set of L frequency-domain transmitted symbols $\bar{s}^{(pd)}_{((i-1)L+l),n}$, for $1 \leq l \leq L$, and, hence, a set of L frequency-domain received signals, denoted by $\bar{x}^{(pd)}_{((i-1)L+l),n}$, for $1 \leq l \leq L$. Thus, denoting by:

$$\bar{\mathbf{x}}^{(pd)}_{i,n} = [\bar{x}^{(pd)}_{((i-1)L+1),n} \; \bar{x}^{(pd)}_{((i-1)L+2),n} \cdots \bar{x}^{(pd)}_{iL,n}]^T \in \mathbb{C}^{L\times 1} \tag{21}$$

the vector containing the L frequency-domain received signals at the n^{th} subcarrier associated with the frequency domain information symbol $\bar{s}_{i,n}$, and assuming that the CFR λ_n ($1 \leq n \leq N$) and PA coefficients c_{2k+1} ($0 \leq k \leq K$) are time-invariant over L symbol periods, we obtain from (7) and (20):

$$\bar{\mathbf{x}}^{(pd)}_{i,n} = \lambda_n \mathbf{W} \bar{\boldsymbol{\phi}}_{i,n} + \bar{\mathbf{v}}^{(pd)}_{i,n}, \tag{22}$$

where $\bar{\mathbf{v}}^{(pd)}_{i,n} \in \mathbb{C}^{L\times 1}$ is the noise vector and $\mathbf{W} = \mathbf{P}\,\mathrm{diag}\,[\,\mathbf{c}\,] \in \mathbb{C}^{L\times(K+1)}$, with:

$$\mathbf{P} = \begin{bmatrix} P_1^{\frac{1}{2}} & \cdots & P_1^{\frac{2K+1}{2}} \\ \vdots & \ddots & \vdots \\ P_L^{\frac{1}{2}} & \cdots & P_L^{\frac{2K+1}{2}} \end{bmatrix} \in \mathbb{C}^{L\times(K+1)}. \tag{23}$$

From (22), it can be concluded that the proposed transmission scheme induces L subchannels, each subchannel being associated with one transmission power. The matrix $\mathbf{W}$ can be expressed as $\mathbf{W} = \mathrm{diag}[P_1^{1/2} \cdots P_L^{1/2}]\,\mathbf{P}_V\,\mathrm{diag}\,[\,\mathbf{c}\,]$, where $\mathbf{P}_V$ is a $L \times (K+1)$ Vandermonde matrix with generators $P_1, P_2, ..., P_L$. The matrix $\mathbf{P}_V$ is full rank if it has distinct generators [37], that is, if $P_i \neq P_j$, for $1 \leq i \neq j \leq L$. As $P_i \neq 0$, for $i = 1, ..., L$, the matrix $\mathrm{diag}[P_1^{1/2} \cdots P_L^{1/2}]$ is full rank as well. Moreover, if $c_{2k+1} \neq 0$ for $0 \leq k \leq K$, the matrix $\mathrm{diag}\,[\,\mathbf{c}\,]$ is also full rank. Thus, if $P_i \neq P_j$, for $1 \leq i \neq j \leq L$ and $c_{2k+1} \neq 0$ for $0 \leq k \leq K$, the matrix $\mathbf{W}$ is full rank. If, in addition, $L \geq (K+1)$, the induced multi-channel representation allows a perfect recovery of $\bar{s}_{i,n}$ in the noiseless case.

The main drawback of this approach is that the transmission rate is divided by L. However, if the PA is modeled by a third-order polynomial ($K = 1$) we can use $L = 2$, which minimizes the transmission rate decrease.

B. PDR with Channel State Information (PDR-CSI)

In this subsection, we propose a technique for nonlinear ICI cancellation, called PDR with Channel State Information (PDR-CSI), assuming that the wireless CFR and PA coefficients are known at the

receiver. Each frequency-domain information symbol is estimated as a linear combination of the received signals, in the following form:

$$\hat{\bar{s}}_{i,n} = \mathbf{g}_n^{(mmse)^T} \bar{\mathbf{x}}_{i,n}^{(pd)}, \tag{24}$$

for $1 \leq n \leq N$, where the vector $\mathbf{g}_n^{(mmse)} \in \mathbb{C}^{L\times 1}$ containing the coefficients of the PDR is calculated by minimizing the mean square error (MSE) cost function:

$$J_n = \mathbb{E}\left[\left|\bar{s}_{i,n} - \mathbf{g}_n^T \bar{\mathbf{x}}_{i,n}^{(pd)}\right|^2\right], \tag{25}$$

which leads to:

$$\mathbf{g}_n^{(mmse)} = \left[\lambda_n^* \mathbf{r}_{\bar{\phi}\bar{s}}^H \mathbf{W}^H \left(\mathbf{W}\mathbf{R}_{\bar{\phi}}\mathbf{W}^H |\lambda_n|^2 + \mathbf{I}_L \sigma^2\right)^{-1}\right]^T, \tag{26}$$

where $\mathbf{R}_{\bar{\phi}} = \mathbb{E}[\bar{\boldsymbol{\phi}}_{i,n}\bar{\boldsymbol{\phi}}_{i,n}^H] \in \mathbb{C}^{(K+1)\times(K+1)}$ is the covariance matrix of the vector $\bar{\boldsymbol{\phi}}_{i,n} \in \mathbb{C}^{(K+1)\times 1}$, $\mathbf{r}_{\bar{\phi}\bar{s}} = \mathbb{E}[\bar{\boldsymbol{\phi}}_{i,n}\bar{s}_{i,n}^*] \in \mathbb{C}^{(K+1)\times 1}$ is the cross-correlation vector of the information symbol with the vector $\bar{\boldsymbol{\phi}}_{i,n}$. Moreover, we have $[\mathbf{R}_{\bar{\phi}}]_{k_1+1,k_2+1} = r_n(k_1,k_2)$ and $[\mathbf{r}_{\bar{\phi}\bar{s}}]_{k_1+1} = r_n(k_1,0)$, for $0 \leq k_1, k_2 \leq K$. The elements of $\mathbf{R}_{\bar{\phi}}$ and $\mathbf{r}_{\bar{\phi}\bar{s}}$ are given by (16) and (18) for $K = 1$, with $r_n(0,0) = \mu_2$.

C. PDR with No Channel State Information (PDR-NCSI)

The technique for nonlinear ICI cancellation presented in the sequel, called PDR with No Channel State Information (PDR-NCSI), assumes that the wireless CFR and PA coefficients are unknown at the receiver. As the MMSE receiver (26) requires the knowledge of the CFR and PA coefficients, the proposed PDR-NCSI is based on a zero-forcing (ZF) strategy that allows to jointly estimate the information symbols and the wireless CFR, by using pilot symbols allocated to subcarriers regularly spaced in the channel passband.

Noting that $\bar{s}_{i,n} = [\bar{\boldsymbol{\phi}}_{i,n}]_1$, the ZF receiver, obtained by solving (22) in the least squares (LS) sense, gives $\hat{\bar{s}}_{i,n} = \mathbf{g}_n^{(zf)^T} \bar{\mathbf{x}}_{i,n}^{(pd)}$, with:

$$\mathbf{g}_n^{(zf)} \;\; = \;\; \lambda_n^{-1} \tilde{\mathbf{w}} \in \mathbb{C}^{L\times 1}, \tag{27}$$

where $\tilde{\mathbf{w}} = [\mathbf{W}^\dagger]_{1,\cdot}^T \in \mathbb{C}^{L\times 1}$. Using the fact that $\mathbf{W} = \mathbf{P}\,\mathrm{diag}\,[\mathbf{c}]$, the ZF solution (27) can be written as:

$$\mathbf{g}_n^{(zf)} = \frac{[\mathbf{P}^\dagger]_{1,\cdot}^T}{\lambda_n c_1}\ . \tag{28}$$

The PDR-NCSI is summarized in Table I, $\hat{\bar{z}}_{i,n}$ being the estimate of $\bar{z}_{i,n} = \bar{s}_{i,n}\lambda_n$. Without loss of generality, we assume that $c_1 = 1$. Moreover, it is assumed that pilot symbols are allocated to a set of D subcarriers, denoted by $\mathcal{N} = \{n_1, \cdots, n_D\}$, regularly spaced in the channel passband. Step 1 amounts to a channel linearization, as it separates the data symbols from the nonlinear ICI, without removing

TABLE I

PDR WITH NO CHANNEL STATE INFORMATION (PDR-NCSI)

1) For $1 \leq n \leq N$, calculate: $\hat{\bar{z}}_{i,n} = [\mathbf{P}^{\dagger}]_{1,\cdot}\, \bar{\mathbf{x}}_{i,n}^{(pd)}$.

2) Estimate the CFR coefficients associated with the pilot subcarriers as:

$$\hat{\lambda}_n = \frac{\hat{\bar{z}}_{i,n}}{\bar{s}_{i,n}},$$

for $n \in \mathcal{N}$.

3) Calculate the CFR coefficients associated with the other subcarriers ($\hat{\lambda}_n$ for $n \notin \mathcal{N}$) by interpolating the CFR coefficients of the pilot subcarriers ($\hat{\lambda}_n$ for $n \in \mathcal{N}$) obtained in Step 2.

4) Estimate the data symbols as:

$$\hat{\bar{s}}_{i,n} = \frac{\hat{\bar{z}}_{i,n}}{\hat{\lambda}_n},$$

for $n \notin \mathcal{N}$.

the multiplicative factor λ_n. Step 2 provides the estimation of the CFR coefficients associated with the pilot subcarriers, while Step 3 interpolates the wireless CFR coefficients of the other sub-carriers from the estimated channel coefficients of the pilot sub-carriers. Several interpolation methods can be used. In our simulations, we applied a DFT interpolation algorithm [38]. Finally, in Step 4, the factor λ_n is removed from $\hat{\bar{z}}_{i,n}$. Steps 2, 3 and 4 correspond to a standard method for estimating and canceling the CFR coefficients from the received signals using a 1-tap receiver to get an estimate of the data symbols.

Remarks:

1) The PDR-NCSI does not need knowledge of the PA coefficients nor the noise variance.
2) For stationary channels, that is, assuming that the CFR and PA coefficients are time-invariant over IL symbol periods, Steps 2 and 3 of the PDR-NCSI can be skipped for $i = 2, \ldots, I$, since the CFR is estimated during the first L symbol periods ($i = 1, .., L$). In this case, pilot subcarriers are used only during the initialization.
3) In the case where $K + 1 = L = 2$, the PDR-NCSI technique needs the computation of only one inverse matrix of dimensions 2×2.
4) After some manipulations, it can be shown that the MMSE and ZF solutions (26) and (27) are equivalent when $\sigma^2 = 0$ and $\mathbf{P}$ is a non-singular matrix. However, when the noise variance is high,

the ZF receiver provides a worst performance with respect to the MMSE receiver due to noise amplification.

D. PDR with Partial CSI (PDR-PCSI)

The last proposed receiver, called PDR with Partial CSI (PDR-PCSI), assumes that the wireless CFR is unknown at the receiver, but the PA coefficients are known. In this case, the PA coefficients are estimated by the transmitter and this information is sent to the receiver through a control channel. The transmission of these parameters must be included in the system initialization. This scheme was used by other authors for OFDM systems [18].

The PDR-PCSI exploits the knowledge of the PA coefficients to improve the performance of the PDR-NCSI. The PDR-PCSI uses an initial estimate of the wireless CFR $\hat{\lambda}_n^{(0)}$ $(1 \leq n \leq N)$ calculated by means of the PDR-NCSI and, then, it iteratively re-estimates the wireless CFR and information symbols by using the MMSE solution. The PDR-PCSI is summarized in Table II. In Step 2, the data symbols are estimated by means of the MMSE method. Step 3 projects the estimated data symbols onto the symbol alphabet to obtain estimates of the nonlinear ICI, which are used in Step 4 to re-estimate the CFR coefficients associated with the pilot subcarriers by means of the LS solution of (22), where $\bar{\phi}_{i,n}$ is replaced by its estimate $\hat{\bar{\phi}}_{i,n}^{(it)}$. In Step 5, the CFR coefficients of the other sub-carriers are estimated by interpolating the channel coefficients of the pilot sub-carriers. Finally, Step 6 checks the algorithm convergence.

As the PDR-PCSI is based on the MMSE solution, it should outperform the PDR-NCSI when the noise power is high. However, the PDR-PCSI is more computationally complex than the PDR-NCSI. In our simulations, the PDR-PCSI converges after a few iterations (less than 5 iterations in the most part of the simulations).

V. POWER FACTORS OPTIMIZATION

In this section, the power factors $P_1, P_2, ..., P_L$ are optimized by minimizing the sum of the residual MSE provided by the proposed PDRs. For simplicity reasons, we consider the case where $K+1 = L = 2$. The problem then consists in finding the values of P_1 and P_2 that minimize: $\sum_{n=1}^{N} J_n$, with J_n defined in (25) and $K = 1$, $\mathbf{g}_n$ being given either by the MMSE solution (26), or by the ZF solution (27), and $0 < P_1, P_2 \leq P_{sat}$, P_{sat} being the input saturation power.

Substituting (26) into (25), we can write the sum of the residual MSE provided by the MMSE receiver

TABLE II

PDR WITH PARTIAL CHANNEL STATE INFORMATION (PDR-PCSI)

- *Initialization ($it = 0$):* Estimate $\hat{\lambda}_n^{(0)}$, for $1 \leq n \leq N$, using Steps 1, 2 and 3 of the PDR-NCSI.
- *Iterations:*

1) $it = it + 1$.
2) For $1 \leq n \leq N$, estimate $\hat{\bar{s}}_{i,n}^{(it)}$ from (24) and (26), using $\hat{\lambda}_n^{(it-1)}$.
3) For $1 \leq n \leq N$, project $\hat{\bar{s}}_{i,n}^{(it)}$ onto the symbol alphabet and construct:
$$\hat{\bar{\boldsymbol{\phi}}}_{i,n}^{(it)} = \left[\hat{\bar{s}}_{i,n}^{(it)} \quad [\bar{\boldsymbol{\psi}}_3(\mathbf{F}^*\hat{\bar{\mathbf{s}}}^{(it)}(i))]_n \ \cdots [\bar{\boldsymbol{\psi}}_{2K+1}(\mathbf{F}^*\hat{\bar{\mathbf{s}}}^{(it)}(i))]_n\right]^T,$$
using the projected symbols.
4) Estimate the CFR coefficients associated with the pilot subcarriers as:
$$\hat{\lambda}_n^{(it)} = \left[[\hat{\mathbf{u}}_{i,n}^{(it)}]^H \bar{\mathbf{x}}_{i,n}^{(pd)}\right] \frac{1}{[\hat{\mathbf{u}}_{i,n}^{(it)}]^H \hat{\mathbf{u}}_{i,n}^{(it)}}, \tag{29}$$
for $n \in \mathcal{N}$, where $\hat{\mathbf{u}}_{i,n}^{(it)} = \mathbf{W}\hat{\bar{\boldsymbol{\phi}}}_{i,n}^{(it)}$.
5) Calculate the CFR of the other subcarriers ($\hat{\lambda}_n$ for $n \notin \mathcal{N}$) by interpolating the CFR of the pilot subcarriers ($\hat{\lambda}_n$ for $n \in \mathcal{N}$) obtained in Step 4.
6) If $\sum_{n=1}^{N} |\hat{\lambda}_n^{(it)} - \hat{\lambda}_n^{(it-1)}|^2 / \sum_{n=1}^{N} |\hat{\lambda}_n^{(it-1)}|^2 < \epsilon$, stop. Otherwise, go to Step 1.

as:

$$J^{(mmse)}(P_1, P_2) = \sum_{n=1}^{N} J_n^{(mmse)}(P_1, P_2) = \sum_{n=1}^{N} \left(\mu_2 - \mathbf{r}_{\bar{\mathbf{x}}\bar{s},n}^H \mathbf{R}_{\bar{\mathbf{x}},n}^{-1} \mathbf{r}_{\bar{\mathbf{x}}\bar{s},n}\right), \tag{30}$$

where $\mathbf{R}_{\bar{\mathbf{x}},n} = \mathbb{E}\left[\bar{\mathbf{x}}_{i,n}^{(pd)} (\bar{\mathbf{x}}_{i,n}^{(pd)})^H\right] \in \mathbb{C}^{L\times L}$ and $\mathbf{r}_{\bar{\mathbf{x}}\bar{s},n} = \mathbb{E}[\bar{\mathbf{x}}_{i,n}^{(pd)} \bar{s}_{i,n}^*] \in \mathbb{C}^{L\times 1}$. In Appendix A, it is demonstrated that, for a high SNR, the absolute minima of (30) in $0 < P_1, P_2 \leq P_{sat}$ are given by: $P_1 = P_{sat}$, $P_2 = \left(\sqrt[3]{\frac{1+\sqrt{3}}{4}} + \sqrt[3]{\frac{1-\sqrt{3}}{4}}\right) P_{sat} \cong 0.313 P_{sat}$ and $P_1 = \left(\sqrt[3]{\frac{1+\sqrt{3}}{4}} + \sqrt[3]{\frac{1-\sqrt{3}}{4}}\right) P_{sat} \cong 0.313 P_{sat}$, $P_2 = P_{sat}$.

On the other hand, substituting (27) into (25), we get for the ZF receiver:

$$J^{(zf)}(P_1, P_2) = \sum_{n=1}^{N} J_n^{(zf)}(P_1, P_2) = \sum_{n=1}^{N} \mathbb{E}\left[\left|\bar{s}_{i,n} - \tilde{\mathbf{w}}^T \mathbf{W} \bar{\boldsymbol{\phi}}_{i,n} - \lambda_n^{-1} \tilde{\mathbf{w}}^T \bar{\mathbf{v}}_{i,n}^{(pd)}\right|^2\right], \tag{31}$$

When $P_1 \neq P_2$, we have $\tilde{\mathbf{w}}^T \mathbf{W} = [1 \quad 0 \quad \ldots \quad 0] \in \mathbb{R}^{1\times(K+1)}$, which leads to:

$$J^{(zf)}(P_1, P_2) = \|\tilde{\mathbf{w}}\|^2 \sum_{n=1}^{N} \frac{\sigma^2}{|\lambda_n|^2}, \tag{32}$$

where $\|\cdot\|$ is the Euclidean norm. In Appendix B, it is demonstrated that the absolute minima of (32) in $0 < P_1, P_2 \leq P_{sat}$ are the same as for the MMSE case.

An important conclusion that can be drawn from the above results is that the optimal transmission powers for the proposed PDRs are constant, i.e. they do not depend on the CFR, nor the PA coefficients and noise variance. On the other hand, if no ICI cancellation is done, the optimal transmission powers depend on the channel and noise conditions [33], [34]. This property constitutes a remarkable advantage of the proposed receivers, as we assumed that the CSI is not available at the transmitter.

VI. Simulation Results

In this section, the proposed receivers are evaluated by means of computer simulations. An OFDM system with a third-degree polynomial PA whose coefficients are equal to $c_1 = 0.9798 - 0.2887\jmath$ and $c_3 = -0.2901 + 0.4350\jmath$ [11], and a wireless link with frequency selective Rayleigh fading due to multipath propagation has been considered for the simulations. The channel impulse response has 4 independent taps and the length of the cyclic prefix is equal to 3 sampling periods ($M_{cp} = M = 3$). The results were obtained with $N = 64$ subcarriers, 16 of them being allocated to pilot symbols, and, when not stated otherwise, with BPSK (binary phase shift keying) transmitted signals. The results represent an average over a large number of independent channel and noise realizations.

In all the simulations, a repetition factor $L = 2$ was used, with the transmission powers obtained in Section V, and, for a given SNR, the noise variance is the same for all the tested techniques. In the figures, the displayed SNR corresponds to the mean SNR at the channel output considering a linear PA, that is, with $c_1 = 0.9798 - 0.2887\jmath$ and $c_3 = 0$, and a transmission power equivalent to $IBO = 10dB$ in the nonlinear PA.

A. Channel Estimation

The next two figures illustrate the channel estimation results, the receivers performance being evaluated by means of the normalized mean square error (NMSE) of the estimated wireless CFR, defined as $NMSE = \frac{1}{N_R}\sum_{i=1}^{N_R} \parallel \mathbf{\Lambda} - \hat{\mathbf{\Lambda}}^{(i)} \parallel_F^2 \; / \; \parallel \mathbf{\Lambda} \parallel_F^2$, where $\hat{\mathbf{\Lambda}}^{(i)} \in \mathbb{C}^{N\times N}$ represents the estimate of $\mathbf{\Lambda}$ at the i^{th} Monte Carlo simulation, $\parallel \cdot \parallel_F$ is the Frobenius norm, and N_R is the number of Monte Carlo simulations.

Fig. 2 shows the CFR NMSE versus SNR provided by the proposed PDR-NCSI and a technique denoted by 1TapRec-NCSI, which corresponds to Steps 2, 3 and 4 of the PDR-NCSI in Table I. This receiver is a standard method for OFDM systems with linear PAs that estimates and cancels the CFR coefficient λ_n from the received signals using a 1-tap receiver. We have tested the 1TapRec-NCSI for several values of IBO. Fig. 2 also shows the CFR NMSE provided by the 1TapRec-NCSI in the case

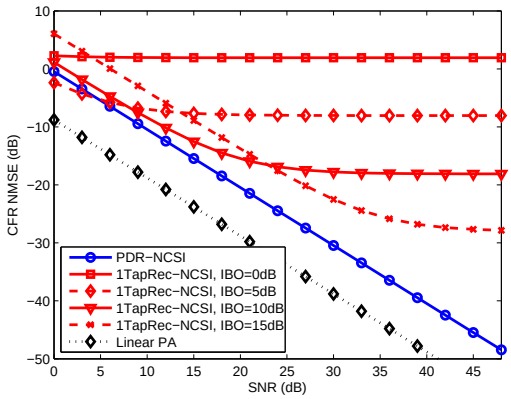

Fig. 2. CFR NMSE versus SNR provided by the PDR-NCSI and 1TapRec-NCSI, for several IBO values.

of a linear PA, that is, with $c_1 = 0.9798 - 0.2887j$ and $c_3 = 0$. It can be concluded that the proposed receiver provides smaller NMSEs than the 1TapRec-NCSI, with no steady floor on the NMSE for high SNRs. This is due to the fact that the optimal transmission powers of the PDRs do not depend on the channel nor the PA coefficients. Moreover, as expected, when the PA is linear, the NMSE is lower than the one obtained with the nonlinear PA. Note also that the NMSE curve of the PDR-NCSI has the same slope than the one obtained with the linear PA.

We have also compared the performance of the PDR-PCSI with that of the technique presented in [18], [32], called power amplifier nonlinearity cancellation (PANC), with frequency domain channel estimation. This technique assumes that the receiver has a PCSI knowledge. Fig. 3 shows the CFR NMSE versus SNR provided by the proposed PDR-PCSI and the PANC-PCSI, the last one being tested with several values of IBO. From these simulation results, we can conclude that the proposed receiver provides better performance, specially for high SNRs.

B. Data Symbol Estimation

In the next five figures, the data symbol estimation precision obtained with the proposed receivers is evaluated by means of the bit-error-rate (BER). Fig. 4 shows the BER versus SNR provided by the proposed PDR-NCSI and the 1TapRec-NCSI, the case of a linear PA being also considered. Fig. 5 shows the BER versus SNR provided by the PDR-PCSI and the PANC-PCSI. The 1TapRec-NCSI and PANC-PCSI techniques were tested with several values of IBO. It can be concluded that the PDRs provide lower BERs than the 1TapRec-NCSI and PANC-PCSI techniques. As for the channel estimation results, there is no saturation on the BER for high SNRs for the proposed receivers, contrary to the 1TapRec-NCSI

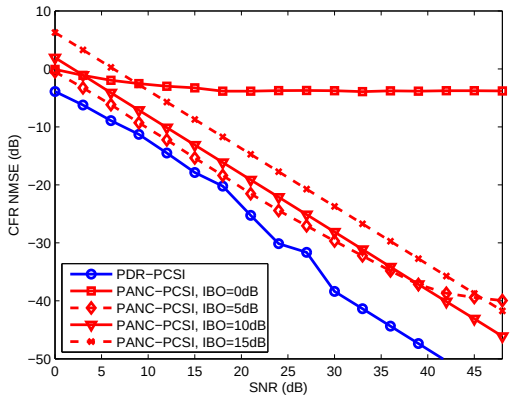

Fig. 3. CFR NMSE versus SNR provided by the PDR-PCSI and PANC-PCSI, for several IBO values.

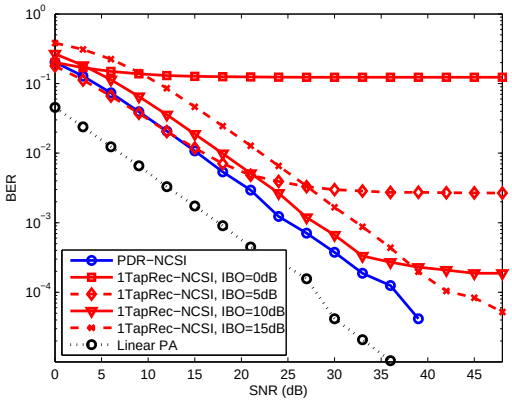

Fig. 4. BER versus SNR provided by the PDR-NCSI and 1TapRec-NCSI.

and PANC-PCSI for $IBO = 0dB$, $5dB$ and $10dB$. Once again, this is due to the fact that the optimal transmission powers of the PDRs do not depend on the channel nor the PA coefficients. Note also that the BER curves of the PDR-NCSI and linear PA have the same slope.

In Figs. 6 and 7, it is considered that the receiver has CSI. Fig. 6 shows the BER versus SNR provided by the PDR-CSI and the 1TapRec-CSI, while Fig. 7 shows the BER versus SNR provided by the PDR-CSI and the PANC assuming CSI, the 1TapRec-CSI and PANC-CSI being tested with several values of IBO. Fig. 6 also shows the BER provided by the 1TapRec-CSI in the case of a linear PA. Once again, the proposed receiver provides lower BERs than the other two receivers. However, in this case, the BER gains of the PDR-CSI with respect to the two other techniques are higher than the one of Figs. 4 and 5. Besides, the SNR loss of the PDR-CSI with respect to the linear PA case is smaller than in Fig. 4.

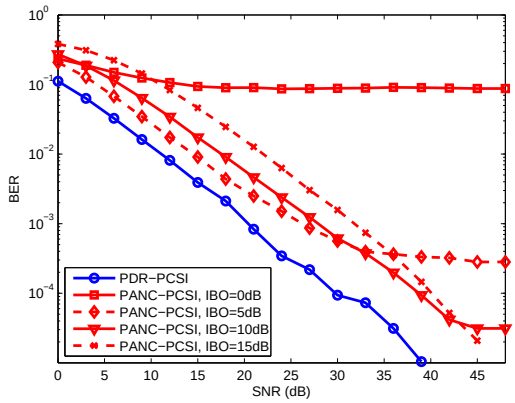

Fig. 5. BER versus SNR provided by the PDR-PCSI and PANC-PCSI.

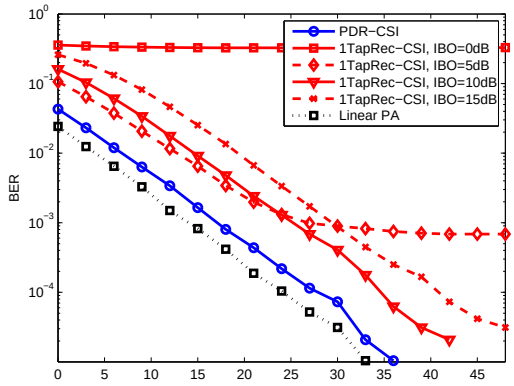

Fig. 6. BER versus SNR provided by the PDR-CSI and 1TapRec-CSI.

Fig. 8 compares the BER provided by the proposed PDRs assuming NCSI, PCSI and CSI, for several Q-QAM constellations. It can be viewed that all the curves have approximately the same slope for high SNRs. Besides, for a $BER = 10^{-3}$ and 2-QAM (BPSK) input, the PDR-CSI has SNR gains of 3.3dB and 7.9dB with respect to the PDR-PCSI and the PDR-NCSI, respectively. For 16-QAM and 64-QAM, the SNR gains of the PDR-CSI with respect to the PDR-PCSI and PDR-NCSI are higher than with 2-QAM. Moreover, for a $BER = 10^{-3}$, the PDR-CSI with 2-QAM has SNR gains of 14.6dB and 20.6dB with respect to the cases of 16-QAM and 64-QAM, respectively.

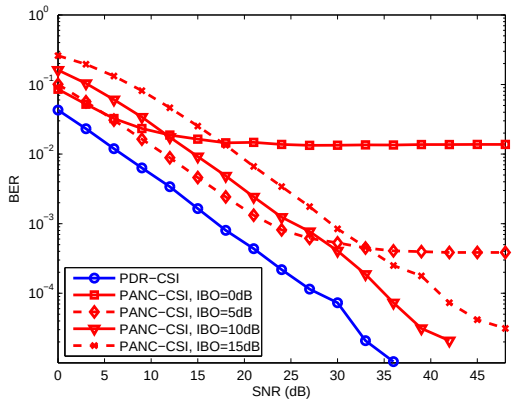

Fig. 7. BER versus SNR provided by the PDR-CSI and PANC-CSI.

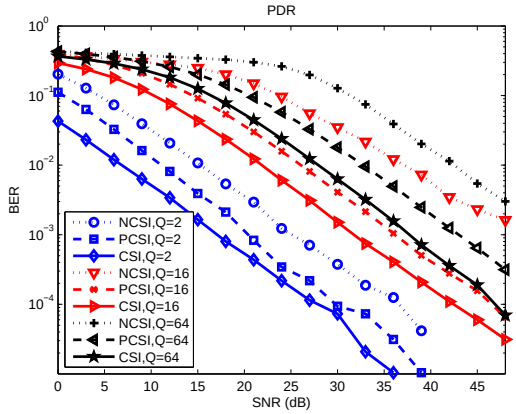

Fig. 8. BER versus SNR provided by the PDR-NCSI, PDR-PCSI and PDR-CSI, for several Q-QAM constellations.

VII. Conclusion

The first contribution of this paper is the theoretical analysis of ICI in nonlinear OFDM systems with polynomial PAs. Contrary to previous works, this analysis provides an exact description of the nonlinear ICI.

The second contribution of the paper is the proposition of three new receivers for ICI cancellation in OFDM systems with polynomial PAs. These receivers consider three different scenarios regarding the CSI at the receiver and are based on the concept of power diversity that consists in re-transmitting the information symbols several times with different transmission powers. Optimal power factors that minimize the sum of the residual MSE provided by the proposed receivers have also been derived in the

case of a third-degree polynomial PA and a repetition factor equal to 2. An important advantage of the proposed receivers is that the optimal transmission powers are constant, i.e. they do not depend on the CFR, nor the PA coefficients and noise variance.

The proposed receivers were tested by means of computer simulations. The simulation results show that the proposed receivers improve the channel estimation and symbol recovery with respect to a standard OFDM receiver and to another technique proposed in the literature. The simulation results also show that the fact that the optimal PDR transmission powers are constant is an important feature of the proposed techniques that leads to a non-saturation on the BER and NMSE for high SNRs. We can then conclude that the proposed PDRs improve the transmission robustness of nonlinear OFDM systems with respect to the tested techniques, at the cost of a reduced spectral efficiency.

The PDR-NCSI can be easily extended to the case of multiple-input multiple-output (MIMO) OFDM systems and to the case of more general PA models, as well as to OFDM systems with cooperative diversity. These extensions will constitute the topics for future works, as well as the power factors optimization for $L > 2$.

APPENDIX A
POWER FACTORS OPTIMIZATION FOR THE MMSE RECEIVER

In this section, we consider the case $K = 1$ and $L = 2$. Let us define: $\mathbf{p}_l = [\mathbf{P}]_{l,\cdot}^T = [P_l^{\frac{1}{2}} \quad P_l^{\frac{3}{2}}]^T \in \mathbb{R}^{2\times 1}$, for $l = 1, 2$, $\bar{\mathbf{u}}_{i,n} = \text{diag}\,[\,\mathbf{c}\,]\,\bar{\boldsymbol{\phi}}_{i,n} \in \mathbb{C}^{2\times 1}$ and $\mathbf{R}_{\bar{\mathbf{u}}} = \mathbb{E}[\bar{\mathbf{u}}_{i,n}\bar{\mathbf{u}}_{i,n}^H] = \text{diag}\,[\,\mathbf{c}\,]\,\mathbf{R}_{\bar{\phi}}\,\text{diag}\,[\,\mathbf{c}^*\,] \in \mathbb{C}^{2\times 2}$, with:

$$\mathbf{R}_{\bar{\phi}} = \mathbb{E}[\bar{\boldsymbol{\phi}}_{i,n}\bar{\boldsymbol{\phi}}_{i,n}^H] = \begin{bmatrix} \mu_2 & r(0,1) \\ r(0,1) & r(1,1) \end{bmatrix} \in \mathbb{C}^{2\times 2}, \tag{33}$$

with $r(0,1)$ and $r(1,1)$ given in (16) and (18), respectively.

From (22), we can express $\mathbf{R}_{\bar{\mathbf{x}},n} = \mathbb{E}\left[\bar{\mathbf{x}}_{i,n}^{(pd)}(\bar{\mathbf{x}}_{i,n}^{(pd)})^H\right] \in \mathbb{C}^{2\times 2}$ and $\mathbf{r}_{\bar{\mathbf{x}}\bar{s},n} = \mathbb{E}[\bar{\mathbf{x}}_{i,n}^{(pd)}\bar{s}_{i,n}^*] \in \mathbb{C}^{2\times 1}$ as:

$$\mathbf{R}_{\bar{\mathbf{x}},n} = |\lambda_n|^2 \begin{bmatrix} \mathbf{p}_1^T\mathbf{R}_{\bar{\mathbf{u}}}\mathbf{p}_1 + \frac{\sigma^2}{|\lambda_n|^2} & \mathbf{p}_1^T\mathbf{R}_{\bar{\mathbf{u}}}\mathbf{p}_2 \\ \mathbf{p}_2^T\mathbf{R}_{\bar{\mathbf{u}}}\mathbf{p}_1 & \mathbf{p}_2^T\mathbf{R}_{\bar{\mathbf{u}}}\mathbf{p}_2 + \frac{\sigma^2}{|\lambda_n|^2} \end{bmatrix} \tag{34}$$

and

$$\mathbf{r}_{\bar{\mathbf{x}}\bar{s},n} = \lambda_n \begin{bmatrix} \mathbf{p}_1^T \\ \mathbf{p}_2^T \end{bmatrix} \mathbf{r}_{\bar{\mathbf{u}}\bar{s}}, \tag{35}$$

with $\mathbf{r}_{\bar{\mathbf{u}}\bar{s}} = \text{diag}\,[\,\mathbf{c}\,]\,\mathbf{r}_{\bar{\phi}\bar{s}} \in \mathbb{C}^{2\times 1}$ and $\mathbf{r}_{\bar{\phi}\bar{s}} = \mathbb{E}[\bar{\boldsymbol{\phi}}_{i,n}\bar{s}_{i,n}^*] = [\mu_2 \;\; r(0,1)]^T \in \mathbb{C}^{2\times 1}$.

Moreover, from (34), we have:

$$\mathbf{R}_{\bar{\mathbf{x}},n}^{-1} = \frac{|\lambda_n|^2}{\det\left[\mathbf{R}_{\bar{\mathbf{x}},n}\right]} \begin{bmatrix} \mathbf{p}_2^T\mathbf{R}_{\bar{\mathbf{u}}}\mathbf{p}_2 + \frac{\sigma^2}{|\lambda_n|^2} & -\mathbf{p}_1^T\mathbf{R}_{\bar{\mathbf{u}}}\mathbf{p}_2 \\ -\mathbf{p}_2^T\mathbf{R}_{\bar{\mathbf{u}}}\mathbf{p}_1 & \mathbf{p}_1^T\mathbf{R}_{\bar{\mathbf{u}}}\mathbf{p}_1 + \frac{\sigma^2}{|\lambda_n|^2} \end{bmatrix} \tag{36}$$

where

$$\det\left[\mathbf{R}_{\bar{\mathbf{x}},n}\right] = |\lambda_n|^4 \left[\left(\mathbf{p}_1^T\mathbf{R}_{\bar{\mathbf{u}}}\mathbf{p}_1 + \frac{\sigma^2}{|\lambda_n|^2}\right)\left(\mathbf{p}_2^T\mathbf{R}_{\bar{\mathbf{u}}}\mathbf{p}_2 + \frac{\sigma^2}{|\lambda_n|^2}\right) - \left(\mathbf{p}_1^T\mathbf{R}_{\bar{\mathbf{u}}}\mathbf{p}_2\right)\left(\mathbf{p}_2^T\mathbf{R}_{\bar{\mathbf{u}}}\mathbf{p}_1\right)\right]. \tag{37}$$

Let us recall that the residual MSE of the n^{th} subcarrier for the MMSE receiver is given by: $J_n^{(mmse)}(P_1,P_2) = \mu_2 - \mathbf{r}_{\bar{\mathbf{x}}\bar{s},n}^H\mathbf{R}_{\bar{\mathbf{x}},n}^{-1}\mathbf{r}_{\bar{\mathbf{x}}\bar{s},n}$. Using (36), $J_n^{(mmse)}(P_1,P_2)$ can be rewritten as:

$$\begin{aligned} J_n^{(mmse)}(P_1,P_2) &= \mu_2 - \left[\mathbf{r}_{\bar{\mathbf{u}}\bar{s}}^H\mathbf{p}_1\mathbf{p}_2^T\mathbf{R}_{\bar{\mathbf{u}}}\mathbf{p}_2\mathbf{r}_{\bar{\mathbf{u}}\bar{s}}^T\mathbf{p}_1 + \mathbf{r}_{\bar{\mathbf{u}}\bar{s}}^H\mathbf{p}_1\mathbf{r}_{\bar{\mathbf{u}}\bar{s}}^T\mathbf{p}_1\frac{\sigma^2}{|\lambda_n|^2} - \mathbf{r}_{\bar{\mathbf{u}}\bar{s}}^H\mathbf{p}_2\mathbf{p}_2^T\mathbf{R}_{\bar{\mathbf{u}}}\mathbf{p}_1\mathbf{r}_{\bar{\mathbf{u}}\bar{s}}^T\mathbf{p}_1 \right. \\ &- \left. \mathbf{r}_{\bar{\mathbf{u}}\bar{s}}^H\mathbf{p}_1\mathbf{p}_1^T\mathbf{R}_{\bar{\mathbf{u}}}\mathbf{p}_2\mathbf{r}_{\bar{\mathbf{u}}\bar{s}}^T\mathbf{p}_2 + \mathbf{r}_{\bar{\mathbf{u}}\bar{s}}^H\mathbf{p}_2\mathbf{p}_1^T\mathbf{R}_{\bar{\mathbf{u}}}\mathbf{p}_1\mathbf{r}_{\bar{\mathbf{u}}\bar{s}}^T\mathbf{p}_2 + \mathbf{r}_{\bar{\mathbf{u}}\bar{s}}^H\mathbf{p}_2\mathbf{r}_{\bar{\mathbf{u}}\bar{s}}^T\mathbf{p}_2\frac{\sigma^2}{|\lambda_n|^2}\right]\frac{|\lambda_n|^4}{\det\left[\mathbf{R}_{\bar{\mathbf{x}},n}\right]}. \end{aligned} \tag{38}$$

On the other hand, by defining $\Gamma_1 = \mathbf{r}_{\bar{\mathbf{u}}\bar{s}}^H\mathbf{p}_1\mathbf{p}_2^T\mathbf{R}_{\bar{\mathbf{u}}}\mathbf{p}_2\mathbf{r}_{\bar{\mathbf{u}}\bar{s}}^T\mathbf{p}_1 - \mathbf{r}_{\bar{\mathbf{u}}\bar{s}}^H\mathbf{p}_2\mathbf{p}_2^T\mathbf{R}_{\bar{\mathbf{u}}}\mathbf{p}_1\mathbf{r}_{\bar{\mathbf{u}}\bar{s}}^T\mathbf{p}_1$, we have:

$$\begin{aligned} \Gamma_1 &= P_1^{\frac{1}{2}}P_2^{\frac{1}{2}}(P_1-P_2)\mathbf{r}_{\bar{\mathbf{u}}\bar{s}}^H\begin{bmatrix} 0 & -1 \\ 1 & 0 \end{bmatrix}\mathbf{R}_{\bar{\mathbf{u}}}^T\mathbf{p}_2\mathbf{r}_{\bar{\mathbf{u}}\bar{s}}^T\mathbf{p}_1 \\ &= \alpha P_1P_2^2(P_1-P_2)\left[\mu_2 + \frac{c_3}{c_1}r(0,1)P_1\right], \end{aligned} \tag{39}$$

where $\alpha = |c_1c_3|^2[r^2(0,1) - \mu_2 r(1,1)]$.

Similarly, defining $\Gamma_2 = -\mathbf{r}_{\bar{\mathbf{u}}\bar{s}}^H\mathbf{p}_1\mathbf{p}_1^T\mathbf{R}_{\bar{\mathbf{u}}}\mathbf{p}_2\mathbf{r}_{\bar{\mathbf{u}}\bar{s}}^T\mathbf{p}_2 + \mathbf{r}_{\bar{\mathbf{u}}\bar{s}}^H\mathbf{p}_2\mathbf{p}_1^T\mathbf{R}_{\bar{\mathbf{u}}}\mathbf{p}_1\mathbf{r}_{\bar{\mathbf{u}}\bar{s}}^T\mathbf{p}_2$ and $\Gamma_3 = \mathbf{r}_{\bar{\mathbf{u}}\bar{s}}^H\mathbf{p}_1\mathbf{r}_{\bar{\mathbf{u}}\bar{s}}^T\mathbf{p}_1\frac{\sigma^2}{|\lambda_n|^2} + \mathbf{r}_{\bar{\mathbf{u}}\bar{s}}^H\mathbf{p}_2\mathbf{r}_{\bar{\mathbf{u}}\bar{s}}^T\mathbf{p}_2\frac{\sigma^2}{|\lambda_n|^2}$, we can write:

$$\Gamma_2 = \mathbf{r}_{\bar{\mathbf{u}}\bar{s}}^H\left(\mathbf{p}_2\mathbf{p}_1^T - \mathbf{p}_1\mathbf{p}_2^T\right)\mathbf{R}_{\bar{\mathbf{u}}}^T\mathbf{p}_1\mathbf{r}_{\bar{\mathbf{u}}\bar{s}}^T\mathbf{p}_2 = -\alpha P_1^2P_2(P_1-P_2)\left[\mu_2 + \frac{c_3}{c_1}r(0,1)P_2\right] \tag{40}$$

and

$$\begin{aligned} \Gamma_3 &= \mathbf{r}_{\bar{\mathbf{u}}\bar{s}}^H\left(\mathbf{p}_1\mathbf{p}_1^T + \mathbf{p}_2\mathbf{p}_2^T\right)\mathbf{r}_{\bar{\mathbf{u}}\bar{s}}\frac{\sigma^2}{|\lambda_n|^2} \\ &= \left[\left|c_1\mu_2P_1^{\frac{1}{2}} + c_3r(0,1)P_1^{\frac{3}{2}}\right|^2 + \left|c_1\mu_2P_2^{\frac{1}{2}} + c_3r(0,1)P_2^{\frac{3}{2}}\right|^2\right]\frac{\sigma^2}{|\lambda_n|^2} \end{aligned} \tag{41}$$

where Re[·] denotes the real part of the argument.

Moreover, we have:

$$\begin{aligned}\frac{\det\left[\mathbf{R}_{\bar{\mathbf{x}},n}\right]}{|\lambda_n|^4} &= P_1^{\frac{1}{2}}P_2^{\frac{1}{2}}(P_1-P_2)\mathbf{p}_1^T\mathbf{R}_{\bar{\mathbf{u}}}\begin{bmatrix}0 & -1\\ 1 & 0\end{bmatrix}\mathbf{R}_{\bar{\mathbf{u}}}^T\mathbf{p}_2+\left(\mathbf{p}_1^T\mathbf{R}_{\bar{\mathbf{u}}}\mathbf{p}_1+\mathbf{p}_2^T\mathbf{R}_{\bar{\mathbf{u}}}\mathbf{p}_2\right)\frac{\sigma^2}{|\lambda_n|^2}+\frac{\sigma^4}{|\lambda_n|^4}\\ &= -\alpha P_1P_2(P_1-P_2)^2+\left[(P_1+P_2)|c_1|^2\mu_2+2(P_1^2+P_2^2)\mathrm{Re}[c_1^*c_3]r(0,1)\right.\\ &+ \left.(P_1^3+P_2^3)|c_3|^2r(1,1)\right]\frac{\sigma^2}{|\lambda_n|^2}+\frac{\sigma^4}{|\lambda_n|^4}. \end{aligned} \quad (42)$$

Thus, substituting (39), (40), (41) and (42) into (38), we get:

$$J_n^{(mmse)}(P_1,P_2)=\mu_2-\frac{\Theta_n(P_1,P_2)}{\frac{\Theta_n(P_1,P_2)}{\mu_2}-\frac{\alpha}{|c_1|^2\mu_2}(P_1^3+P_2^3)\frac{\sigma^2}{|\lambda_n|^2}+\frac{\sigma^4}{|\lambda_n|^4}}, \quad (43)$$

with

$$\begin{aligned}\Theta_n(P_1,P_2) = -\alpha P_1P_2(P_1-P_2)^2\mu_2+\left[\left|c_1\mu_2P_1^{\frac{1}{2}}+c_3r(0,1)P_1^{\frac{3}{2}}\right|^2\right.\\ \left.+\left|c_1\mu_2P_2^{\frac{1}{2}}+c_3r(0,1)P_2^{\frac{3}{2}}\right|^2\right]\frac{\sigma^2}{|\lambda_n|^2}. \end{aligned} \quad (44)$$

Assuming that $\Theta_n(P_1,P_2)\neq 0$, we can then express $J_n^{(mmse)}(P_1,P_2)$ as:

$$J_n^{(mmse)}(P_1,P_2)=\mu_2-\frac{1}{\frac{1}{\mu_2}+\frac{-\frac{\alpha}{|c_1|^2\mu_2}(P_1^3+P_2^3)\frac{\sigma^2}{|\lambda_n|^2}+\frac{\sigma^4}{|\lambda_n|^4}}{\Theta_n(P_1,P_2)}}. \quad (45)$$

Minimizing (45) is equivalent to minimizing:

$$\tilde{J}_n^{(mmse)}(P_1,P_2)=\frac{-\frac{\alpha}{|c_1|^2\mu_2}(P_1^3+P_2^3)\frac{\sigma^2}{|\lambda_n|^2}+\frac{\sigma^4}{|\lambda_n|^4}}{\Theta_n(P_1,P_2)}. \quad (46)$$

There is no analytical solution for this minimization problem. However, the cost function (46) can be simplified when the SNR $\gamma_n=\mu_2|\lambda_n|^2/\sigma^2$ is high. In this case, (46) can be approximated by:

$$\tilde{J}_n^{(mmse)}(P_1,P_2)\cong\frac{\sigma^2(P_1^3+P_2^3)}{|\lambda_n|^2|c_1|^2r^2(0,0)P_1P_2(P_1-P_2)^2}, \quad (47)$$

whose absolute minimum is given by $P_1=P_{sat}$ and $P_2=(\sqrt[3]{\frac{1+\sqrt{3}}{4}}+\sqrt[3]{\frac{1-\sqrt{3}}{4}})P_{sat}\simeq 0.313P_{sat}$ (or vice-versa). The proof is given in the Lemma of Appendix C. Note that this solution does not depend on the subcarrier number n, which means that it is also the absolute minimum of $J^{(mmse)}(P_1,P_2)=\sum_{n=1}^N J_n^{(mmse)}(P_1,P_2)$ when the SNR γ_n is high.

It should be remarked that (47) is not a good approximation of (46) if $P_1\cong P_2$. However, we have observed in computer simulations that, when the SNR is high, the cost function (46) exhibits very high values when $P_1\cong P_2$. Indeed, we can deduce from (44) that $\Theta_n(P_1,P_1)\cong 0$ when $\sigma^2/|\lambda_n|^2$ is low. This means that, when the SNR is high, (47) is a good approximation of (46) at the neighborhoods of the minima points.

APPENDIX B
POWER FACTORS OPTIMIZATION FOR THE ZF RECEIVER

In this section, we consider the case $K = 1$ and $L = 2$, with $P_1 \neq P_2$. Recalling that $\tilde{\mathbf{w}} \in \mathbb{C}^{2\times 1}$ is the transpose of the first row of the matrix $\mathbf{W}^{\dagger} \in \mathbb{C}^{2\times 2}$, where $\mathbf{W} = \mathbf{P}\,\mathrm{diag}\,[\,\mathbf{c}\,] \in \mathbb{C}^{2\times 2}$, we then have:

$$\tilde{\mathbf{w}} = \frac{1}{P_1^{\frac{1}{2}} P_2^{\frac{1}{2}} (P_2 - P_1) c_1} \begin{bmatrix} P_2^{\frac{3}{2}} \\ -P_1^{\frac{3}{2}} \end{bmatrix}. \tag{48}$$

From (48) and (32), the sum of the residual MSE provided by the ZF receiver can be written as:

$$J^{(zf)}(P_1, P_2) = \frac{(P_1^3 + P_2^3)}{P_1 P_2 (P_2 - P_1)^2 |c_1|^2} \sum_{n=1}^{N} \frac{\sigma^2}{|\lambda_n|^2}, \tag{49}$$

which is proportional to $\tilde{J}^{(mmse)}(P_1, P_2)$ defined in (47). This means that the absolute minimum of $J^{(zf)}(P_1, P_2)$ is given by $P_1 = P_{sat}$ and $P_2 = \left(\sqrt[3]{\frac{1+\sqrt{3}}{4}} + \sqrt[3]{\frac{1-\sqrt{3}}{4}} \right) P_{sat} \cong 0.313 P_{sat}$ (or vice-versa).

APPENDIX C
LEMMA

Let us consider the function $f(x, y) = \frac{x^3+y^3}{xy(x-y)^2}$, with $x, y \in \mathbb{R}$. The absolute minimum of $f(x, y)$ with $0 < y < x \leq X_{\max}$, is given by:

$$(x, y) = \left(X_{\max}, X_{\max} \left(\sqrt[3]{\frac{1+\sqrt{3}}{4}} + \sqrt[3]{\frac{1-\sqrt{3}}{4}} \right) \right). \tag{50}$$

Proof:

The partial derivative of $f(x, y)$ with respect to x is given by:

$$\frac{\partial f(x, y)}{\partial x} = \frac{-2x^3 - 3xy^2 + y^3}{x^2 (x - y)^3}. \tag{51}$$

As $x > y$, we have $-2x^3 + y^2(-3x + y) < 0$, $x^2 (x - y)^3 > 0$ and, hence, $\frac{\partial f(x,y)}{\partial x} < 0$, which means that for $x > y$, $f(x, y)$ is a decreasing function with respect to x. Thus, the minima of $f(x, y)$ with $0 < y < x \leq X_{\max}$ are located on the plane $x = X_{\max}$. Similarly:

$$\frac{df(X_{\max}, y)}{dy} = \frac{-2y^3 - 3yX_{\max}^2 + X_{\max}^3}{y^2 (y - X_{\max})^3}. \tag{52}$$

By making $df(X_{\max}, y)/dy = 0$, we get: $-2y^3 - 3X_{\max}^2 y + X_{\max}^3 = 0$. This equation has only one real root, given by:

$$\hat{y} = X_{\max} \left(\sqrt[3]{\frac{1+\sqrt{3}}{4}} + \sqrt[3]{\frac{1-\sqrt{3}}{4}} \right). \tag{53}$$

Moreover, after some calculations, it can be verified that $\frac{d^2 f(X_{\max},y)}{dy^2}\Big|_{y=\hat{y}} > 0$, which proves that $(X_{\max}, \hat{y})$ is the absolute minimum of $f(x,y)$ in $0 < y < x \leq X_{\max}$.

□

REFERENCES

[1] T. Hwang, C. Yang, G. Wu, S. Li, and G. Y. Li, "OFDM and its wireless applications: a survey," *IEEE Transactions on Vehicular Technology*, vol. 58, no. 4, pp. 1673–1694, May 2009.

[2] R. Prasad, *OFDM for Wireless Communications Systems*, 1st ed. Artech House, Inc., 2004.

[3] E. Costa and S. Pupolin, "M-QAM-OFDM system performance in the presence of a nonlinear amplifier and phase noise," *IEEE Transactions on Communications*, vol. 50, no. 3, pp. 462–472, Mar. 2002.

[4] D. Dardari, V. Tralli, and A. Vaccari, "A theoretical characterization of nonlinear distortion effects in OFDM systems," *IEEE Transactions on Communications*, vol. 48, no. 10, pp. 1755–1764, Oct. 2000.

[5] G. Zhou and R. Raich, "Spectral analysis of polynomial nonlinearity with applications to RF power amplifiers," *EURASIP Journal on Applied Signal Processing*, vol. 12, pp. 1831–1840, 2004.

[6] O. Muta, I. Kaneko, Y. Akaiwa, and H. Furukawa, "Adaptive predistortion linearization based on orthogonal polynomial expansion for nonlinear power amplilfiers in OFDM systems," in *International Conference on Communications and Signal Processing (ICCSP 2011)*, Kerala, India, Feb. 2011, pp. 512–516.

[7] C. Yan, Z. Chun-Hua, Y. Shou-Yi, and X. Hui, "Spectrum analysis of OFDM-based communication systems with nonlinear high power amplifier," in *International Conference on Communications and Mobile Computing*, Shenzhen, China, Apr. 2010, pp. 451–454.

[8] L. Ding, "Digital predistortion of power amplifiers for wireless applications," Ph.D. dissertation, School of Electrical and Computer Engineering, Georgia Institute of Technology, USA, Mar. 2004.

[9] R. Raich, "Nonlinear system identification and analysis with applications to power amplifier modeling and power amplifier predistortion," Ph.D. dissertation, School of Electrical and Computer Engineering, Georgia Institute of Technology, USA, Mar. 2004.

[10] R. Marsalek, "Contributions to the power amplifier linearization using digital baseband adaptive predistortion," Ph.D. dissertation, Université de Marne-la-Vallée, France, 2003.

[11] V. A. Bohara and S. H. Ting, "Theoretical analysis of OFDM signals in nonlinear polynomial models," in *International Conference on Information, Communications and Signal Processing*, Singapore City, Singapore, Dec. 2007, pp. 10–13.

[12] T. Araújo and R. Dinis, "On the accuracy of the gaussian approximation for the evaluation of nonlinear effects in OFDM signals," in *IEEE Vehicular Technology Conference Fall (VTC-Fall)*, Ottawa, Canada, Sept. 2010, pp. 1–5.

[13] P. Banelli, G. Baruffa, and S. Cacopardi, "Effects of HPA nonlinearity on frequency multiplexed OFDM signals," *IEEE Transactions on Broadcasting*, vol. 47, no. 2, pp. 123–136, Jun. 2001.

[14] N. Y. Ermolova, "Analysis of OFDM error rates over nonlinear fading radio channels," *IEEE Transactions on Wireless Communications*, vol. 9, no. 6, pp. 1855–1860, Jun. 2010.

[15] E. Aschbacher, "Digital pre-distortion of microwave power amplifiers," Ph.D. dissertation, Vienna University of Technology, Austria, Sep. 2005.

[16] L. Ding, G. T. Zhou, D. R. Morgan, Z. Ma, J. S. Kenney, J. Kim, and C. R. Giardina, "A robust digital baseband predistorter constructed using memory polynomials," *IEEE Transactions on Communications*, vol. 52, no. 1, pp. 159–165, Jan. 2004.

[17] V. A. Bohara and S. H. Ting, "Analysis of OFDM signals in nonlinear high power amplifier with memory," in *IEEE International Conference on Communications*, Beijing, China, May 2008, pp. 3653–3657.

[18] F. Gregorio, S. Werner, T. I. Laakso, and J. Cousseau, "Receiver cancellation technique for nonlinear power amplifier distortion in SDMA-OFDM systems," *IEEE Transactions on Vehicular Technology*, vol. 56, no. 5, pp. 2499–2516, Sep. 2007.

[19] A. N. D'Andrea, V. Lottici, and R. Reggiannini, "Nonlinear predistortion of OFDM signals over frequency-selective fading channels," *IEEE Transactions on Communications*, vol. 49, no. 5, pp. 837–843, May 2001.

[20] R. Raich, H. Qian, and G. T. Zhou, "Digital baseband predistortion of nonlinear power amplifiers using orthogonal polynomials," in *IEEE International Conference on Acoustics, Speech, and Signal Processing (ICASSP)*, vol. 6, Hong-Kong, Apr. 2003, pp. 689–692.

[21] S. Litsyn, *Peak Power Control in Multicarrier Communications*, 1st ed. Cambridge University Press, 2007.

[22] V. Vijayarangan and R. Sukanesh, "An overview of techniques for reducing peak to average power ratio and its selection criteria for orthogonal frequency division multiplexing radio systems," *Journal of Theoretical and Applied Information Technology*, vol. 5, no. 1, pp. 25–36, Jan. 2009.

[23] I. A. Ulian and A. N. Barreto, "Comparação entre pós- e pré-processamento para a mitigação dos efeitos não lineares em um sistema OFDM," in *Brazilian Telecommunication Symposium*, Curitiba, Brazil, Oct. 2011, pp. 2–5.

[24] J. Yang, X. Mu, S. Yang, L. Qi, and H. Kobayashi, "A compensation method for nonlinear distortion in OFDM system," in *International Conference on Advanced Communication Technology*, Phoenix Park, Korea, Feb. 2007, pp. 881–884.

[25] N. Ermolova, "OFDM equalization in nonlinear time-varying channels," in *International Symposium on Wireless Communication Systems*, Valencia Spain, Sep. 2006, pp. 358–362.

[26] N. Ermolova, N. Nefedov, and S. Haggman, "An iterative method for non-linear channel equalization in OFDM systems," in *IEEE International Symposium on Personal, Indoor and Mobile Radio Communications*, vol. 1, Barcelona, Spain, Sep. 2004, pp. 484–488.

[27] H. Chen and A. Haimovich, "Iterative estimation and cancellation of clipping noise for OFDM signals," *IEEE Communications Letters*, vol. 7, no. 7, pp. 305–307, Jul. 2003.

[28] C. Xia and J. Ilow, "Blind compensation of memoryless nonlinear effects in OFDM transmissions using CDF," in *Communication Networks and Services Research Conference*, Moncton, Canada, May 2003.

[29] A. J. Redfern and G. T. Zhou, "Nonlinear channel identification and equalization for OFDM systems," in *IEEE International Conference on Acoustics, Speech and Signal Processing (ICASSP)*, vol. 6, Seattle, WA,USA, May 1998, pp. 3521–3524.

[30] S. Chang and E. J. Powers, "Cancellation of inter-carrier interference in OFDM systems using a nonlinear adaptive filter," in *IEEE International Conference on Communications (ICC)*, New Orleans, LA , USA, Jun. 2000, pp. 1039–1043.

[31] F. Gregorio, "Analysis and compensation of nonlinear power amplifiers effects in multi-antenna OFDM systems," Ph.D. dissertation, Helsinki University of Technology, Finland, 2007.

[32] J. Tellado, L. Hoo, and J. Cioffi, "Maximum-likelihood detection of nonlinearly distorted multicarrier symbols by iterative decoding," *IEEE Transactions on Communications*, vol. 51, no. 2, pp. 218–228, Feb. 2003.

[33] M. Senst and G. Ascheid, "Optimal output back-off in OFDM systems with nonlinear power amplifiers," in *IEEE International Conference on Communications (ICC)*, Dresden, Germany, Jun. 2009, pp. 1–6.

[34] T. Riihonen, S. Werner, F. Gregorio, R. Wichman, and J. Hamalainen, "BEP analysis of OFDM relay links with nonlinear power amplifiers," in *IEEE Wireless Communications and Networking Conference (WCNC)*, Sydney, Australia, Apr. 2010, pp. 1–6.

[35] C. A. R. Fernandes, J. C. M. Mota, and G. Favier, "MIMO Volterra modeling for nonlinear communication channels," *Learning and Nonlinear Models*, vol. 2, no. 8, pp. 71–92, Dec. 2010.

[36] R. M. Gray, "Toeplitz and circulant matrices: A review," *Foundations and Trends in Communications and Information Theory*, vol. 2, no. 3, pp. 155–239, 2005.

[37] N. D. Sidiropoulos and X. Liu, "Identifiability results for blind beamforming in incoherent multipath with small delay spread," *IEEE Transactions on Signal Processing*, vol. 49, no. 1, pp. 228–236, Jan. 2001.

[38] K. P. Prasad and P. Satyanarayana, "Fast interpolation algorithm using FFT," *Electronics Letters*, vol. 22, no. 6, pp. 185–187, Feb. 1986.